

Cascaded H-bridge Multilevel PV Inverter with Fuzzy Logic Controller for Grid Connected Systems

Sk. Basha Mohiddin, M. Kishore

Abstract— A modular cascaded H-bridge multilevel photovoltaic (PV) inverter with Fuzzy Logic Controller for three-phase grid-connected applications is presented in this paper. This topology helps to enhance the flexibility and efficiency of PV inverter systems. Due to the PV mismatches, unbalanced current is injected into the grid which leads to many power quality issues. Modulation compensation scheme is proposed in the control scheme of inverter to eliminate the adverse effects of PV mismatches. A distributed maximum power point tracking scheme is applied to inverter topology for better utilization and to maximize the solar energy extraction from PV modules. For efficacious functioning of cascaded inverter, Fuzzy logic controller is utilized in the control scheme. To verify the feasibility of the proposed approach, a three phase seven level cascaded multilevel inverter is modeled and simulation results are presented by utilizing MATLAB/SIMULINK.

Index Terms— Photovoltaic (PV), Distributed maximum power point (MPP) tracking (MPPT), modulation compensation, Fuzzy Logic Controller (FLC), Membership Functions, Fuzzification, Defuzzification.

I. INTRODUCTION

Renewable energy technologies are clean sources of energy that have a much lower environmental impact than conventional energy technologies. There are many types of renewable energy sources. Among them, solar energy plays a key role in the power generation sector. The demand for the solar energy has increased by 20%–25% for every annum over the span of late 20 years [1], and the development is for the most part in Grid connected systems. With the rapid market development in photovoltaic (PV) systems, there is incrementing scope for grid connected Photovoltaic applications.

There are five types of inverter topologies related to different PV system configurations namely: 1) central inverters; 2) string inverters; 3) multistring inverters; 4) ac-module inverters; and 5) cascaded inverters [2]–[7]. These PV system topologies are shown in Fig. 1. Cascaded inverter comprises of number of converters connected in series and are commonly used in medium and large scale grid-connected PV applications [8]–[10]. Since the converters are connected in

series, high power and/or high voltage is available without the necessity of boosting stages. Cascaded inverter topologies are categorized into two types.

A cascaded dc/dc converter connection of PV modules is presented in Fig. 1(e) [11], [12]. Each dc/dc converter is fed by an individual dc source, and these dc/dc converter modules are connected in series to produce a high dc voltage, which is supplied to a simplified dc/ac inverter.

This methodology cumulates features of string inverters and ac-module inverters and adds the advantage of distributed maximum power point (MPP) tracking (MPPT), yet it is not so much expensive but rather more efficient than ac-module inverters. Moreover, it consists of two power conversion stages in this topology.

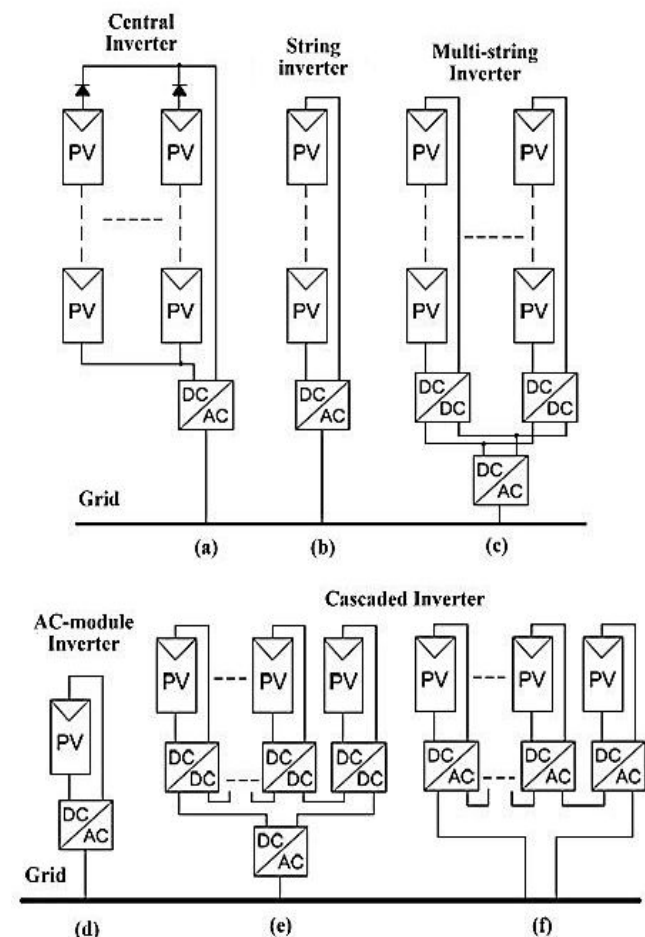


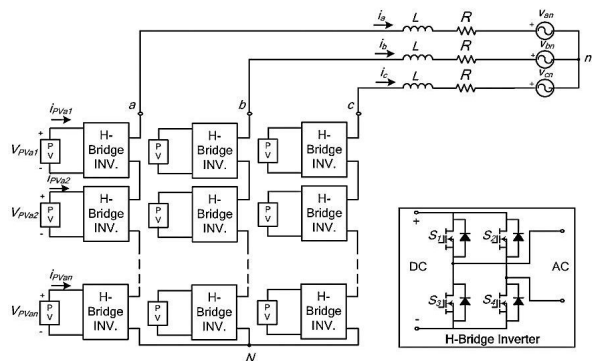
Fig. 1. PV inverter topologies. (a) Central inverter. (b) String inverter. (c) Multistring inverter. (d) AC-module inverter. (e) Cascaded dc/dc converter. (f) Cascaded dc/ac inverter.

Manuscript received July 22, 2016

Sk. Basha Mohiddin, M.Tech degree in Solar Power Systems from Madanapalle Institute of Technology and Science, Madanapalle, Andhra Pradesh, India

M. Kishore, Assistant professor in Madanapalle Institute of Technology Science, Madanapalle, Andhra Pradesh, India

The other cascaded topology is presented in Fig. 1(f), in which each PV panel is associated to a dc/ac inverter. Those inverters are then connected in series to make up a high-voltage level [13]–[16]. This cascaded inverter has the advantages of better utilization per PV module, capability of combining different sources, redundancy of the system and improvement of efficiency of the PV system.



A fuzzy logic controller controlled cascaded multilevel inverter for grid-connected applications are presented in this paper. The issues regarding panel mismatch in a grid connected system are addressed, and to eliminate these issues a control scheme with distributed MPPT control is proposed. Besides, if each PV panel has at its own Maximum Power Point, unbalanced current is injected into the grid which leads to power quality problems. Modulation compensation is additionally integrated to the control system to balance the three-phase grid current. Integral action of PI controller inverse the oscillatory and rolling behavior of PV panels and it is arduous to arrive the best tuning values. PI controller has maximum overshoot and high settling time. Fuzzy logic controllers have superior performance than PI controllers. Hence for efficacious functioning of cascaded inverter Fuzzy Logic Controller is employed in the control scheme. To validate the developed control scheme, simulation results are presented by utilizing MATLAB/SIMULINK.

II. SYSTEM DESCRIPTION

A three-phase grid connected Modular cascaded H-bridge multilevel photovoltaic inverter topology is shown in Fig. 2. This topology comprises of n H-bridge converters connected in series in each phase. An individual solar PV panel or a short string of PV panels is utilized to feed the dc link of each H-bridge. The cascaded multilevel inverter is connected to the grid by using Inductor filters, which are adapted to minimize the switching harmonics in the current. The four switches in each H-bridge module are switched in different combinations to create three output voltage levels namely: $-V_{dc}$, 0, or $+V_{dc}$. Since the cascaded multilevel inverter topology consists of n input sources in each phase, the ac output waveform is synthesized with $(2n + 1)$ levels.

The size of the filters required for the reduction of the harmonics in the synthesized current reduces due to this $(2n + 1)$ level output voltage waveform. The other benefits of multilevel inverters include reduced voltage stresses on the

semiconductor switches and having higher efficiency when compared to other grid connected converter topologies [17].

III. PANEL MISMATCHES

Due the dissimilar irradiance and temperatures and aging of the PV panels, PV mismatch is a major problem which commonly occurs in the PV system. Due to this, the MPP of each PV panel might be distinctive. The efficiency of the overall PV system will be decremented if each PV module is not controlled individually.

PV mismatch may cause more difficulties in a three-phase grid-connected PV system. In addition to decrementing the overall efficiency, this could even introduce unbalanced power supplied to the three-phase grid-connected system.

The input power of each phase would be different if there are PV mismatches between phases. This difference in input power will cause unbalanced current to the grid, which is not acceptable by grid standards. For example, to unbalance the current per phase more than 10% is not allowed for some utilities, where the percentage imbalance is calculated by taking the difference between the maximum deviation of current and the average current and dividing it by the average current [18].

To overcome the PV mismatch problem, distributed MPPT and modulation compensation scheme is included in the proposed control scheme. The control scheme details will be discussed in the following section.

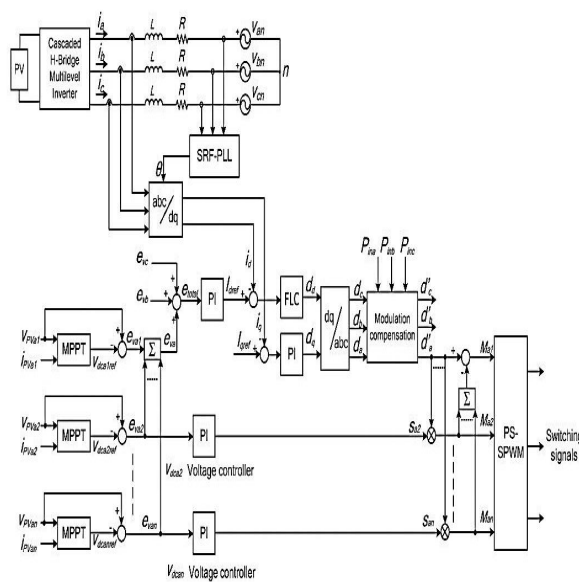


Fig. 3. Control scheme of inverter with distributed MPPT and modulation compensation scheme

IV. CONTROL SCHEME

A. Distributed MPPT Control

To improve the efficiency of the PV system and to eliminate the adverse effect of the mismatches, the PV modules need to work at different voltages to enhance the usage per PV module. The cascaded H-bridge multilevel inverter has separate dc links which makes independent voltage control possible. The control scheme proposed in [19]

is updated for this application to implement individual MPPT control in each PV module.

A three-phase cascaded H-bridge inverter with distributed MPPT control is shown in Fig. 3. A MPPT controller is integrated in each H-bridge module to generate the dc-link voltage reference. Each dc-link voltage and the corresponding voltage reference are compared, and these errors are added and controlled through a total voltage controller that determines the current reference I_{dref} . The reactive current reference I_{qref} can be set to zero, or if reactive power emolument is required, I_{qref} can withal be given by a reactive current calculator [20], [21]. The phase-locked loop (PLL) has been utilized to find the phase angle of the grid voltage [22]. In the control scheme of the three-phase systems, the grid currents in abc coordinates are converted to dq coordinates and regulated through Fuzzy Logic Controller (FLC) to generate the modulation index in the dq coordinates, which is then converted back to three phases.

To make each PV module operate at its own MPP, take phase a as an example; the voltages V_{dca2} to $V_{dca n}$ are controlled individually through $n - 1$ loops. Each voltage controller gives the modulation index proportion of one H-bridge module in phase a. After multiplied by the modulation index of phase a, $n - 1$ modulation indices can be obtained. Additionally, the modulation index for the first H-bridge can be obtained by subtraction.

The control schemes in phases b and c are nearly same. The only distinction is that all dc-link voltages are regulated through PI controllers, and n modulation index proportions are acquired for each phase.

A phase-shifted sinusoidal pulse width modulation switching scheme is then applied to control the switches of each H-bridge. There are many MPPT methods have been developed for PV systems [23], [24]. For Maximum Power Point Tracking, the Incremental Conductance technique has been utilized as a part of this paper.

B. Fuzzy Logic Controller

The PWM Control goes the objective is to control the flow of electrical energy between source and load by controlling the inverter. Despite of how many controllers and control loops, it has the only quantity that may be controlled is the magnitude of the inverter output voltage and its frequency. The higher the voltage the better and more faster the energy becomes. The advantage of fuzzy logic controller is it doesn't require models and can be utilized in nonlinear process and it has high performance than PI controllers.

The fundamental architecture of the FLC utilized as a part of the control strategy is shown in Fig. 4. The main components that make up a FLC system are the fuzzifier unit at the input terminal, Knowledge base (rule base) and the inference engine, and defuzzifier at the output terminal. In FLC predicated control system, the required variables are the input and output variables. The inputs to the FLC are the parameters or variables of the process to be controlled which depend on the applications. Customarily an error and its rate of change are chosen for the input variables. Meanwhile, the change in gain of modulation index is culled as the output variables. An error in discrete time is the distinction between the desired output or reference, $r(k)$, and the process output

variable, $y(k)$. The current sample of error, $e(k)$ and the change of error $\Delta e(k)$ are defined in (1) and (2), respectively

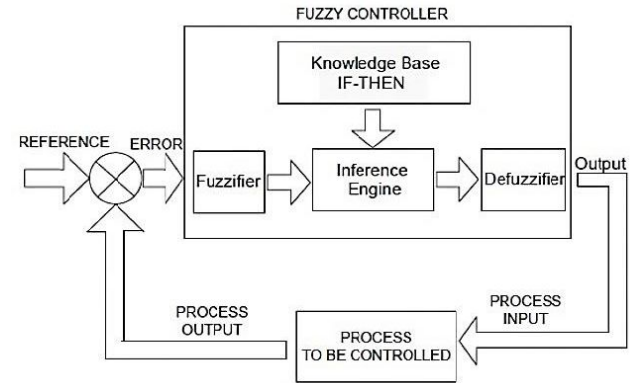


Fig. 4. Fuzzy logic control architecture.

$$e(k) = r(k) - y(k) \quad (1)$$

$$\Delta e(k) = e(k) - e(k - 1) \quad (2)$$

The inputs and output are categorized into four fuzzy subsets: NB (Negative Big), NS (Negative Small), PS (Positive Small) and PB (Positive Big). The fuzzy rules and the membership functions are shown in Fig. 5. The Mamdani FIS system with Max-Min is utilized to operate the fuzzy combination.

	NB	NS	PS	PB
NB	PB	PB	NB	NB
NS	PS	PS	NS	NS
PS	NS	NS	PS	PS
PB	NB	NB	PB	PB

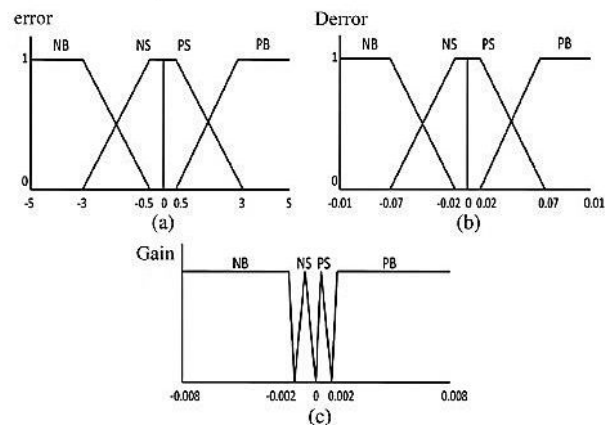


Fig. 5. Membership functions for (a) error, (b) change in error and (c) controller Gain and Rule based matrix table.

By the essence of the inference process and with the aid of the knowledge-based rules, the fuzzy output is generated. The essential part of the FLC is the knowledge-based element, which consists of a list of fuzzy rules [25]. The inference process is to generate a fuzzy output set according to the IF-THEN rules. With these rules, the fuzzy controller behaves

intelligently and capable of imitating humanlike-decision. There are 16 rules of 'IF-THEN' logic related to the inputs and outputs. This logic makes the control function into an FLC.

In the system implementation, the fuzzy controller output, $u(k+1)T_s$, keep changing in every sampling time until it reaches a steady-state condition as described in (3) [26].

$$u(k+1) = u(k) + \Delta u(k) \quad (3)$$

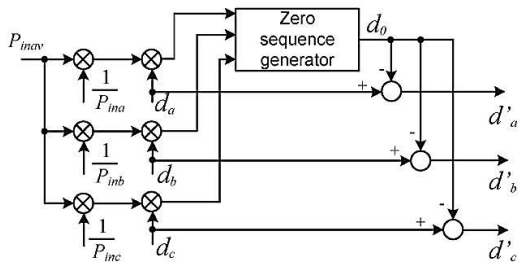
Where, $\Delta u(k)$ is the sample of controller output. In this work, the center of area defuzzification method is used to calculate the actual output from its fuzzy value as given in (4). It is a simple and precise technique which finds the 'balance' point of the solution region by calculating the weighted mean of the fuzzy region.

$$u = \frac{\sum_{i=1}^k w_i \mu(u_i)}{\sum_{i=1}^k \mu(u_i)} \quad (4)$$

Where $\mu(u_i)$ is membership value of the combined membership function corresponding to each rule.

C. Modulation Compensation

In three-phase modular cascaded H-bridge multilevel PV inverter, as specified before, PV mismatches may create more problems. In each H-bridge module, with the distributed MPPT control the solar power of each phase would be distinctive, which introduces unbalanced current to the grid. To solve the issue, a zero sequence voltage can be imposed upon the phase legs in order to affect the current flowing into each phase [27], [28]. If the updated inverter output phase voltage is proportional to the unbalanced power, the current will be balanced.



Thus, the modulation compensation block, as shown in Fig. 6, is integrated to the control scheme of PV inverters. The key is how to update the modulation index of each phase without increasing the complexity of the control system. First, the unbalanced power is biased by ratio r_j , which is calculated as follows

$$r_j = \frac{P_{inav}}{P_{inj}} \quad (5)$$

where P_{inav} is the average input power and P_{inj} is the input power of phase j ($j = a, b, c$). Then, the injected zero sequence modulation index can be generated as

$$d_0 = \frac{2}{3} [\min(r_a \cdot d_a, r_b \cdot d_b, r_c \cdot d_c) + \max(r_a \cdot d_a, r_b \cdot d_b, r_c \cdot d_c)] \quad (6)$$

where d_j is the modulation index of phase j ($j = a, b, c$) and is determined by the current loop controller. The modulation index of each phase is updated by

$$d_j' = d_j - d_0 \quad (7)$$

Only simple calculations are required in the scheme, which will not increase the complexity of the control system. An example is presented to show the modulation compensation scheme more clearly. Assume that the input power of each phase is unequal

$$P_{ina} = 0.8 \quad P_{inb} = 1 \quad P_{inc} = 1. \quad (8)$$

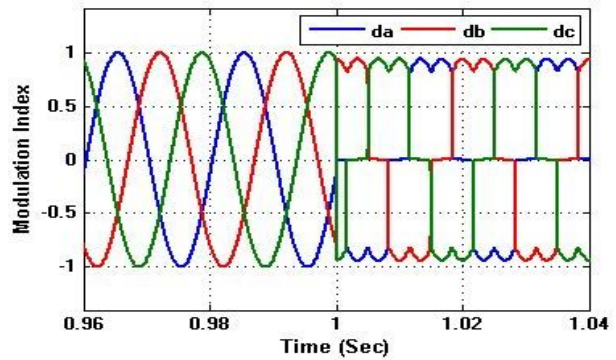


Fig. 7. Modulation indices before and after modulation compensation.

By injecting a zero sequence modulation index at $t = 1$ s, the balanced modulation index will be updated, as shown in Fig. 7. It can be seen that, with the compensation, the updated modulation index is unbalanced proportional to the power, which implies that the output voltage (V_{jn}) of the three-phase inverter is unbalanced; however this produces the desired balanced grid current.

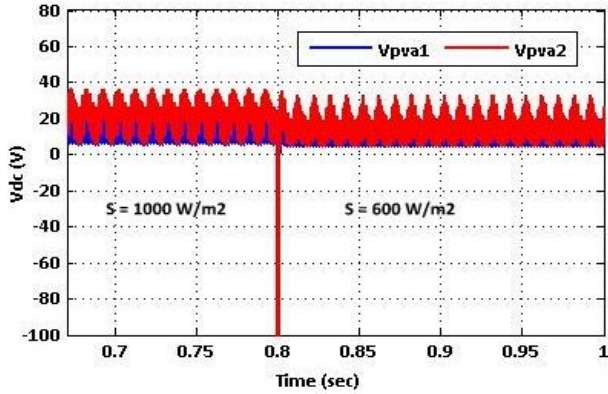
V. SIMULATION RESULTS

A three-phase seven-level cascaded H-bridge multilevel inverter is simulated. Each H-bridge module is fed by an individual PV panel. The inverter is connected to the grid using a transformer whose secondary voltage is 60 Vrms. The system parameters in the PV inverter are shown in Table I.

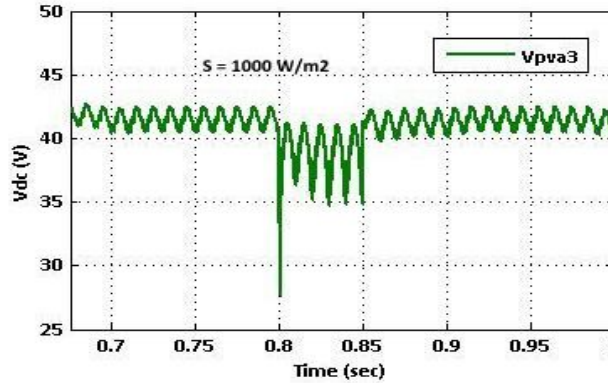
To validate the three-phase grid connected PV inverter with the proposed control scheme, it is simulated in two different environments. First, all PV panels are operated under the same irradiance and temperature at 1000 W/m^2 and 25°C respectively. At $t = 0.8$ s, the solar irradiance decreases to 600 W/m^2 on the first and second panels of phase a, and that for the other panels stays the same as previous environment. Fig. 8 shows the dc-link voltages of phase a. At the starting, all PV panels are operated at an MPP voltage of 38.4 V. As the irradiance changes, the first and second dc link voltages reduce and track the new MPP voltage of 37.2 V, while the third panel is still operated at 38.4V.

TABLE I
 SYSTEM PARAMETERS

Parameters	Value
DC-link Capacitor	3600 μ F
Connection Inductor L	2.5 mH
Grid Resistor R	0.1 Ω
Grid rated Phase Voltage	60 Vrms
Switching Frequency	1.5 kHz



(a)



(b)

Fig. 8. DC-link voltages of phase a with individual MPPT (a) Voltages of modules 1 and 2. (b) Voltage of module 3.

Fig. 9 shows the PV current waveforms of phase a. After $t = 0.8$ s, due to the low irradiance, the currents of the first and second PV panels are much smaller and the lower ripple of the dc-link voltage can be found in Fig. 8(a).

With the distributed MPPT control in each H-bridge, the dc-link voltage of can be controlled independently. This means, the connected PV panel of each H-bridge can be operated at its own MPP voltage and will not be influenced by the panels connected to other H-bridges. Thus, more solar energy can be extracted, and the efficiency of the overall PV system will be incremented.

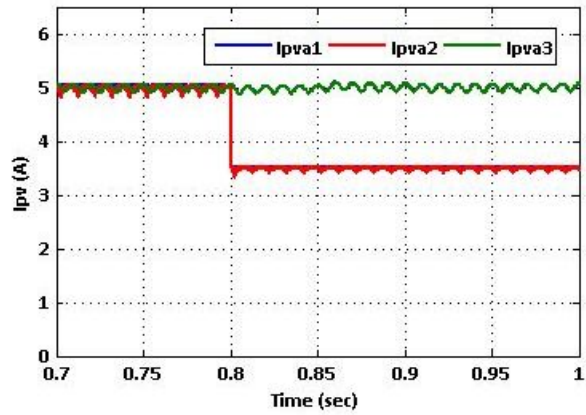


Fig. 9. PV currents of phase a with distributed MPPT.

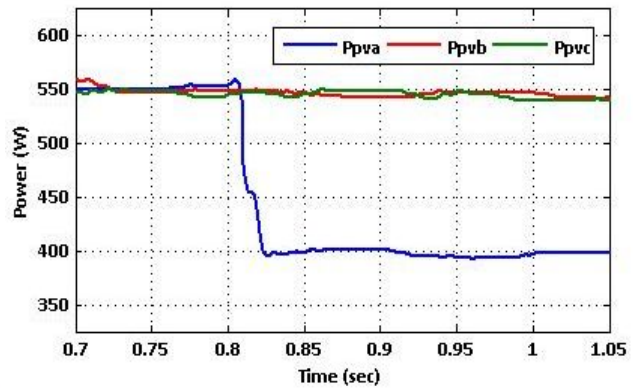


Fig. 10. Power extracted from PV panels with distributed MPPT.

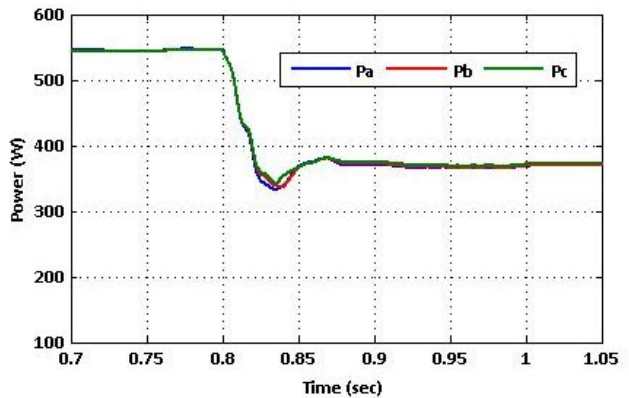


Fig. 11. Power injected to the grid with modulation compensation.

The power extracted from the PV panels from each phase is shown in Fig. 10. At the beginning, all panels are operated under irradiance $S = 1000$ W/m² and every phase is generating a maximum power of 550 W. After $t = 0.8$ s, the power harvested from phase a decreases to 400 W, and those from the other two phases stay the same. Obviously, the power supplied to the three-phase grid-connected inverter is unbalanced. However, by applying the modulation compensation scheme, the power injected to the grid is still balanced, as shown in Fig. 11. Fig. 12 explains the output voltages (V_{jn}) of the three-phase inverter.

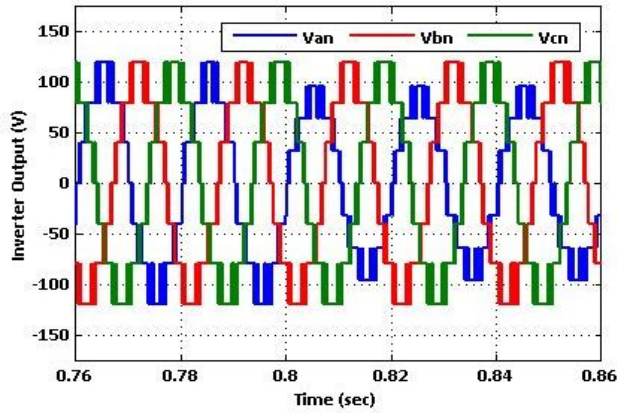


Fig. 12. Three-phase inverter output voltage waveforms with modulation compensation.

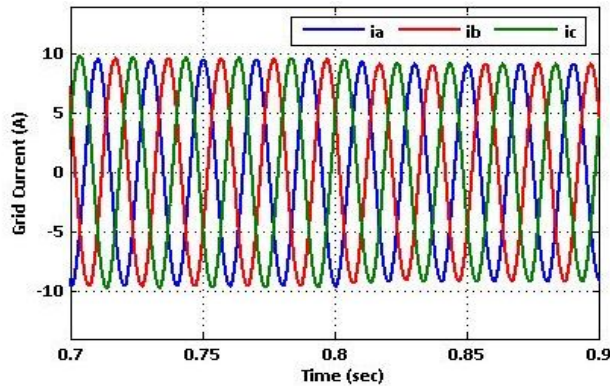


Fig. 13. Three-phase grid current waveforms with modulation compensation.

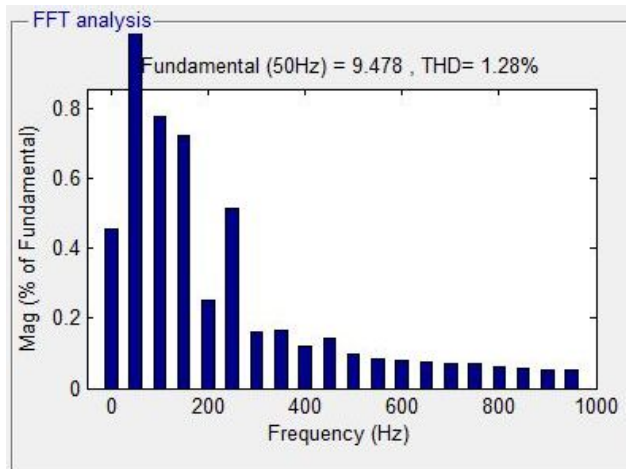


Fig. 14. THD of the grid current shown in Fig. 13.

Due to the injected zero sequence component, they are unbalanced after $t = 0.8$ s, which help to balance the grid current shown in Fig. 13. Fig. 14 shows the THD of the Grid current shown in Fig. 13 and it is calculated as 1.28%. With the proposed control scheme, each PV module can be works at its own MPP to maximize the solar energy extraction, and three phase balanced power is supplied to the Grid.

VI. CONCLUSION

A modular cascaded H-bridge multilevel inverter with fuzzy logic controller for grid-connected PV applications has been presented in this paper. With distributed MPPT scheme,

the multilevel inverter topology enhances the utilization of connected PV modules and increases the overall efficiency of PV systems. PV mismatches may cause unbalanced power supplied to the inverter, resulting in unbalanced injected grid current.

A Modulation compensation scheme, which will not increase the complexity of the control system is added to balance the grid current. By using the Fuzzy Logic Controller in the Control scheme, the inverter is effectively controlled to extract the maximum power from the Solar panels and to supply the power to the Grid. With the proposed control scheme, each PV module can be operated at its own MPP to maximize the solar energy extraction, and the three-phase grid current is balanced even with the unbalanced supplied solar power.

FUTURE WORK

REFERENCES

- [1] J. M. Carrasco et al., "Power-electronic systems for the grid integration of renewable energy sources: A survey," *IEEE Trans. Ind. Electron.*, vol. 53, no. 4, pp. 1002–1016, Jun. 2006.
- [2] S. B. Kjaer, J. K. Pedersen, and F. Blaabjerg, "A review of single-phase grid connected inverters for photovoltaic modules," *IEEE Trans. Ind. Appl.*, vol. 41, no. 5, pp. 1292–1306, Sep./Oct. 2005.
- [3] M. Meinhardt and G. Cramer, "Past, present and future of grid connected photovoltaic and hybrid power-systems," in *Proc. IEEE PES Summer Meet.*, 2000, vol. 2, pp. 1283–1288.
- [4] M. Calais, J. Myrzik, T. Spooner, and V. G. Agelidis, "Inverter for single phase grid connected photovoltaic systems—An overview," in *Proc. IEEE PESC*, 2002, vol. 2, pp. 1995–2000.
- [5] J.M. A. Myrzik and M. Calais, "String and module integrated inverters for single-phase grid connected photovoltaic systems—A review," in *Proc. IEEE Bologna Power Tech Conf.*, 2003, vol. 2, pp. 1–8.
- [6] F. Schimpf and L. Norum, "Grid connected converters for photovoltaic, state of the art, ideas for improvement of transformerless inverters," in *Proc. NORPIE*, Espoo, Finland, Jun. 2008, pp. 1–6.
- [7] B. Liu, S. Duan, and T. Cai, "Photovoltaic DC-building-module-based BIPV system—Concept and design considerations," *IEEE Trans. Power Electron.*, vol. 26, no. 5, pp. 1418–1429, May 2011.
- [8] L. M. Tolbert and F. Z. Peng, "Multilevel converters as a utility interface for renewable energy systems," in *Proc. IEEE Power Eng. Soc. Summer Meet.*, Seattle, WA, USA, Jul. 2000, pp. 1271–1274.
- [9] H. Ertl, J. Kolar, and F. Zach, "A novel multicell DC–AC converter for applications in renewable energy systems," *IEEE Trans. Ind. Electron.*, vol. 49, no. 5, pp. 1048–1057, Oct. 2002.
- [10] S. Daher, J. Schmid, and F. L. M. Antunes, "Multilevel inverter topologies for stand-alone PV systems," *IEEE*

- Trans. Ind. Electron., vol. 55, no. 7, pp. 2703–2712, Jul. 2008.
- [11] G. R. Walker and P. C. Sernia, “Cascaded DC–DC converter connection of photovoltaic modules,” IEEE Trans. Power Electron., vol. 19, no. 4, pp. 1130–1139, Jul. 2004.
- [12] E. Roman, R. Alonso, P. Ibanez, S. Elorduizapatarietxe, and D. Goitia, “Intelligent PV module for grid-connected PV systems,” IEEE Trans. Ind. Electron., vol. 53, no. 4, pp. 1066–1073, Jun. 2006.
- [13] F. Filho, Y. Cao, and L. M. Tolbert, “11-level cascaded H-bridge grid tied inverter interface with solar panels,” in Proc. IEEE APEC Expo., Feb. 2010, pp. 968–972.
- [14] C. D. Townsend, T. J. Summers, and R. E. Betz, “Control and modulation scheme for a cascaded H-bridge multi-level converter in large scale photovoltaic systems,” in Proc. IEEE ECCE, Sep. 2012, pp. 3707–3714.
- [15] B. Xiao, L. Hang, and L. M. Tolbert, “Control of three-phase cascaded voltage source inverter for grid-connected photovoltaic systems,” in Proc. IEEE APEC Expo., Mar. 2013, pp. 291–296.
- [16] Y. Zhou, L. Liu, and H. Li, “A high-performance photovoltaic module integrated converter (MIC) based on cascaded quasi-Z-source inverters (qZSI) using eGaN FETs,” IEEE Trans. Power Electron., vol. 28, no. 6, pp. 2727–2738, Jun. 2013.
- [17] J. Rodriguez, J. S. Lai, and F. Z. Peng, “Multilevel inverters: A survey of topologies, controls, and applications,” IEEE Trans. Ind. Electron., vol. 49, no. 4, pp. 724–738, Aug. 2002.
- [18] Standard for Electric Installation and Use. [Online]. Available: <https://www.xcelenergy.com/>
- [19] A. Dell’Aquila, M. Liserre, V. Monopoli, and P. Rotondo, “Overview of PI-based solutions for the control of DC buses of a single-phase H-bridge multilevel active rectifier,” IEEE Trans. Ind. Appl., vol. 44, no. 3, pp. 857–866, May/Jun. 2008.
- [20] B. Xiao, K. Shen, J. Mei, F. Filho, and L.M. Tolbert, “Control of cascaded H-bridge multilevel inverter with individual MPPT for grid-connected photovoltaic generators,” in Proc. IEEE ECCE, Sep. 2012, pp. 3715–3721.
- [21] Y. Xu, L. M. Tolbert, J. N. Chiasson, F. Z. Peng, and J. B. Campbell, “Generalized instantaneous non-active power theory for STATCOM,” IET Elect. Power Appl., vol. 1, no. 6, pp. 853–861, Nov. 2007.
- [22] V. Kaura and V. Blasko, “Operation of a phase locked loop system under distorted utility conditions,” IEEE Trans. Ind. Appl., vol. 33, no. 1, pp. 58–63, Jan./Feb. 1997.
- [23] T. Esram and P. L. Chapman, “Comparison of photovoltaic array maximum power point tracking techniques,” IEEE Trans. Energy Convers., vol. 22, no. 2, pp. 439–449, Jun. 2007.
- [24] D. P. Hohm and M. E. Ropp, “Comparative study of maximum power point tracking algorithms,” Progr. Photovolt., Res. Appl., vol. 11, no. 1, pp. 47–62, Jan. 2003.
- [25] D.K. Chaturvedi, Modeling and Simulation of Systems Using MATLAB and Simulink, CRC Press, 2006.
- [26] Z. Kovacic, S. Bogdan, Fuzzy Controller Design: Theory and Applications, CRC Press, 2006.
- [27] S. Rivera et al., “Cascaded H-bridge multilevel converter multistring topology for large scale photovoltaic systems,” in Proc. IEEE ISIE, Jun. 2011, pp. 1837–1844.
- [28] T. J. Summers, R. E. Betz, and G. Mirzaeva, “Phase leg voltage balancing of a cascaded H-bridge converter based STATCOM using zero sequence injection,” in Proc. Eur. Conf. Power Electron. Appl., Sep. 2009, pp. 1–10.



Sk. Basha Mohiddin¹ received his B.Tech degree in Electrical and Electronics Engineering from Audisankara Institute of Technology, Gudur in 2014. Presently he is pursuing his M.Tech degree in Solar Power Systems from Madanapalle Institute of Technology and Science, Madanapalle, Andhra Pradesh, India. His areas of interest are Solar Photovoltaic technology and Renewable energy sources.



M. Kishore² received his B.Tech degree in Electrical and Electronics Engineering from Sri Venkateswara College of Engineering and Technology, Chittoor in 2010. He received his M.Tech degree in Power Electronics and Drives from NIT Warangal in 2012. He is currently working as an Assistant professor in Madanapalle Institute of Technology Science, Madanapalle, Andhra Pradesh, India. His areas of interest are Multilevel Inverters and Power Electronics and Drives.